Published in final edited form as:
J Immunol. 2016 December 15; 197(12): 4771–4779. doi:10.4049/jimmunol.1600604.

PTPN22 is a critical regulator of Fcγ receptor mediated neutrophil activation

Sonja Vermeren[*], **Katherine Miles**[*], **Julia Y. Chu**[*], **Donald Salter**[†], **Rose Zamoyska**[‡], and **Mohini Gray**[*]

[*]MRC / UoE Centre for Inflammation Research, Queen's Medical Research Institute, University of Edinburgh, United Kingdom

[†]Institute for Genetics and Molecular Medicine, University of Edinburgh, United Kingdom

[‡]Institute of Immunology and Infection Research, Ashworth Laboratories; University of Edinburgh, United Kingdom

Abstract

Neutrophils act as a first line of defense against bacterial and fungal infections but they are also important effectors of acute and chronic inflammation. Genome wide association studies have established that the gene encoding the protein tyrosine phosphatase PTPN22 makes an important contribution to susceptibility to autoimmune disease, notably rheumatoid arthritis. Although PTPN22 is most highly expressed in neutrophils, its function in these cells remains poorly characterized. We show here that neutrophil effector functions, including adhesion, production of reactive oxygen species and degranulation induced by immobilized immune complexes were reduced in *Ptpn22*$^{-/-}$ neutrophils. Tyrosine phosphorylation of Lyn and Syk was altered in *Ptpn22*$^{-/-}$ neutrophils. On stimulation with immobilized immune complexes, *Ptpn22*$^{-/-}$ neutrophils manifested reduced activation of key signaling intermediates. *Ptpn22*$^{-/-}$ mice were protected from immune complex mediated arthritis, induced by the transfer of arthritogenic serum. In contrast, *in vivo* neutrophil recruitment following thioglycollate induced peritonitis and *in vitro* chemotaxis were not affected by lack of PTPN22. Our data suggest an important role for PTPN22-dependent dephosphorylation events, that are required to enable full Fcγ receptor induced activation, pointing to an important role for this molecule in neutrophil function.

Introduction

Neutrophils are the most abundant peripheral blood leukocytes in humans. As part of the innate immune system they provide an immediate response to infection or injury. Neutrophils are rapidly activated by a variety of stimuli, including bacterial peptides, complement and immune complexes. Autoimmune diseases, including rheumatoid arthritis

Authors for correspondence: Sonja.Vermeren@ed.ac.uk and Mohini.Gray@ed.ac.uk, MRC / UoE Centre for Inflammation Research, Queen's Medical Research Institute, 47 Little France Crescent, Edinburgh EH16 4TJ, U.K. Phone (+44) 131 2429100, Fax (+44) 131 2426578.

Authorship Contributions: SV and MG initiated the study and designed the experiments; SV, KM and YJC performed experiments; SV, KM, YJC, DS and MG analyzed experiments and interpreted the data; RZ provided experimental tools and advice. SV, MG and RZ wrote the manuscript.

Europe PMC Funders Author Manuscripts

(RA), are associated with the generation of immune complexes, that accumulate in synovial fluid or are deposited on articular cartilage surfaces. They engage and activate neutrophils via Fcγ receptors (FcγRs) (1, 2). Severe inflammation follows neutrophil degranulation, releasing a plethora of degradative enzymes and other inflammatory mediators (3). The ensuing release of ROS and proteases degrades articular cartilage, whilst secreted chemokines attract further immune cells into the joint, driving chronic inflammation (4). Thus neutrophilic inflammation forms a crucial part of the inflammatory response, which needs to be resolved in a timely manner to minimize host damage.

Protein tyrosine phosphatase nonreceptor 22 (PTPN22) is a leukocyte-restricted phosphatase, which is associated with an increased risk in a range of autoimmune diseases, notably RA. The single missense nucleotide polymorphism (SNP), C1858T encoding an R620W substitution is the single most important non MHC gene contributor to RA susceptibility, and the second most important for juvenile idiopathic arthritis according to candidate gene and genome wide association studies (5, 6). Although expression of PTPN22 is highest in the neutrophil (7), its function in these myeloid cells remains largely unknown. In T cells, PTPN22 has been shown to suppress T cell receptor (TCR) signaling, for instance by dephosphorylating key tyrosine residues within the activation loops of the Src family kinases (SFKs) Lck and Fyn and the TCR adapter Zap-70. At least in T cells, PTPN22 cooperates with the C-terminal Src kinase (Csk); their physical interaction is critical to their synergistic regulatory function. On a protein level, the disease-associated R620W variant (R619W in the mouse) affects one of four proline-rich regions in the C-terminus of PTPN22. This disrupts PTPN22 binding to Csk (8, 9).

The K/BxN serum transfer arthritis model of arthritis is induced by administration of arthritogenic serum from arthritic KRN x NOD donors. This bypasses the need for an adaptive immune system-driven break in self-tolerance. It results in a transient, but rapidly evolving inflammatory arthritis, that reproduces many of the hallmarks of RA (10, 11). In combination with a range of experimental approaches, including genetic lineage depletion and reconstitutions, this disease model has helped to elucidate the important contribution of innate immune cells, notably neutrophils, to the effector phase of rheumatoid arthritis (12–14).

We present here an analysis of PTPN22 function in the neutrophil, concentrating on FcγR signaling due to its prominent role in autoimmune diseases. By performing functional assays with isolated neutrophils from PTPN22 deficient mice and by analysing inflammation in K/BxN serum transfer arthritis, we demonstrate that PTPN22 regulates FcγR neutrophilic inflammation.

Methods

Unless otherwise stated, materials were obtained from Sigma.

Antibodies

Antibodies directed against phosphotyrosine (PY1000), phospho-Syk (Y525/526), phospho-pan Src (Y527 and Y416), phospho-Akt (S473), phospho-p38 (T180, Y182) and phospho-

Erk (T202, Y204) were from Cell Signaling Technology. Anti-Syk (clone 5F5) and anti-Lyn (clone LYN-01) were from Biolegend. Anti-Ly6G (clone RC6-8C5) was obtained from R&D Systems. Anti-BSA and anti-lactoferrin antibodies were from Sigma and an antibody against β-COP was a gift from Nick Ktistakis (The Babraham Institute, Cambridge). HRP-conjugated secondary antibodies were from Santa Cruz Biotechnology and Biorad. Fluorescently-conjugated antibodies for flow cytometry were obtained from eBioscience (F4/80, GR1), Biolegend (CD11b, CD11a, CD16/32, Ly6G, CD62L, CD19) and BD (Ly6C).

PTPN22 mouse model

Generation of the *PTPN22* mouse has been previously described (15). Experimental mice were housed in individually ventilated cages in a specific and opportunistic pathogen free small animal barrier unit at the University of Edinburgh. All animal work was approved by United Kingdom Home Office Project license PPL60/4567.

Analysis of peripheral blood

Peripheral blood was sampled from the superficial temporal vein into sodium citrate. Leukocytes were stained using fluorescently conjugated antibodies, mixed with flow-check fluorospheres (Beckman Coulter) to determine cell numbers and red blood cells were lysed (BD FacsLyse). Samples were analysed by flow cytometry using a LSR Fortessa (BD).

K/BxN serum transfer arthritis model

The K/BxN serum transfer model was induced using pooled arthritogenic serum as previously described (10, 11, 16). Mice were scored for 20 days. Each limb was scored as; 0, normal; 1, erythema or swelling in a single digit; 2, erythema and swelling in two or more joints; 3, swelling of the entire paw including the hock joint. The sum of the score for each limb (giving a maximum possible score of 12) was taken as a measure of the extent of arthritis at that time-point. Formalin fixed samples were prepared for histology by decalcification in EDTA. 3 μm sections were stained with hematoxillin and eosin. Immunostaining for Ly6G was performed according to standard procedures without antigen retrieval employing a secondary HRP-coupled antibody followed by a DAB reaction. Analysis of histological specimen occurred in a blinded fashion by a histopathologist, using an Olympus BX51 microscope. Images were acquired using a Micropublisher 3.3RTV camera and Q Imaging software using 2x, 20x and 40x objectives.

Thioglycollate induced sterile peritonitis

Sterile peritonitis was induced by injection of matured 4% Brewer's thioglycollate (BD) at a concentration of 20 ml/kg. Mice were sacrificed 3 hours after induction and peritoneal cells harvested following a peritoneal flush. Cells were stained with fluorescently conjugated antibodies and mixed with flow-check fluorospheres (Beckman Coulter) to determine cells numbers, before being analysed by fluorescence activated flow sorting using the LSR Fortessa (BD).

Neutrophil purification

Neutrophils were isolated from bone marrows of 12 to 14 week old sex- and age-matched mice using discontinuous Percoll gradients (GE Healthcare Amersham, Uppsala, Sweden) as previously described (17, 18), using endotoxin-free reagents throughout.

Immobilized immune complexes and immobilization of adhesive proteins

For immobilized immune complexes (ICs), dishes were coated overnight at 4ºC with endotoxin and fatty acid free BSA in PBS (100 μg/ml), blocked with 1% fat free milk in PBS, and incubated with rabbit anti-BSA (1:2000). Control surfaces were treated identically, but not incubated with antibody. Some assays were carried out with insoluble immune complexes, which had been generated as described (19). Human fibrinogen (150 μg/ml), polyRGD (20 μg/ml) or, as a control, heat-inactivated fetal calf serum (HI-FCS) were adsorbed onto tissue culture grade plastics overnight at 4ºC and for 3 hours at room temperature, respectively. All surfaces were extensively washed with PBS prior to performing any assays.

ROS production assays

ROS production was measured by chemiluminescence in a Synergy H1 plate reader (BioTek) employing a luminol-based assay in luminescence grade 96-well plates (Nunc, Thermo Scientific) essentially as previously described (20). Measurements were started immediately following cell stimulation and light emission was recorded. Data output was relative light units per second (RLU/sec).

Chemotaxis assays

For chemotaxis assays, neutrophils were resuspended in HBSS supplemented with 15mM Hepes pH 7.4 and 0.05% fatty acid and endotoxin free BSA. Dunn chambers were assembled as described (21), and chemotaxis assays were carried out employing MIP2 (R&D Systems) as chemoattractant. Cells were monitored by time-lapse imaging for 30 minutes using an inverted RMDIB microscope (Leica) equipped with temperature controlled chamber, automated stage (Prior), Orca camera (Hamamatsu) and Micromanager image acquisition software (Fiji). Paths of all individual neutrophils were tracked using the ‘manual tracking’ plug-in into ImageJ. Tracks were subsequently analysed using the ‘Chemotaxis Tool’ (Ibidi) plug-in into Image J.

Transendothelial migration assays

TEM assays were carried out as previously described (22). Briefly, 6.5μm transwell inserts with 3μm polycarbonate membranes (Costar, Corning, UK) were coated overnight with 2μg/ml fibronectin, and seeded with 5 x 10^4 bEnd5 cells grown in DMEM supplemented with 10% heat inactivated fetal bovine serum (both Life Technologies) as described. Confluent bEnd5 cells were stimulated for 16 hrs with 5nM TNFα and 5 x 10^5 neutrophils were added into washed inserts that had been placed into wells of 24 well plates in the presence of 0, 1 or 3nM MIP2 and allowed to migrate towards the chemoattractant. Transmigrated neutrophils were labelled for GR1 and 8 randomly chosen fields of view / 24

well were photographed for counting [20x magnification using an Evos cell imaging system (AMG)].

Adhesion assays

Neutrophils were allowed to adhere to immobilized IC or blocked surfaces at 37ºC in 96 well plates. Dishes were then subjected to rapid orbital shaking for 30 seconds before contents were flicked sharply out of wells prior to cell fixation. Following extensive washing, 4 random images were taken from each well for analysis of cell spreading (20x magnification; Evos system).

Degranulation assays

Gelatinase granule release after plating neutrophils onto an immobilized IC coated surface, or following stimulation with fMLF and cytochalasin B was detected by in-gel zymography as previously described (20). Lactoferrin release was assayed by making use of an antibody to human lactoferrin that had previously been shown to cross-react with mouse protein essentially as described (23, 24).

Analysis of protein phosphorylation

Neutrophils were plated onto immobilized IC coated or control treated dishes for stimulation. For analysis of phosphorylation of PKB, Erk and p38 MAPK, this was done as previously described (20, 25). For analysis of Lyn and Syk, non-adherent cells and scraped, adherent cells were combined for lysis in ice-cold 100mM NaCl, 30mM Hepes pH7.4, 20mM NaF, 1mM EGTA, 1% Triton X-100, 1mM benzamidine, 10μg/ml aprotinin, 1mM PMSF, 1mM Na_3VO_4 as well as mammalian protease inhibitor cocktail and phosphatase inhibitor cocktail 2. After pelleting detergent-insoluble material, proteins of interest were immunoprecipitated using protein G agarose and antibodies as indicated. Carefully washed beads were boiled in sample buffer and immunoprecipitated proteins and lysate controls separated SDS-PAGE. Proteins were transferred to Immobilon membrane (Millipore) for Western blotting using antibodies as indicated.

Cytokine release assays

Cytokine release assays were carried out using insoluble HSA-anti HSA immune complexes as stimulation. Insoluble ICs were prepared by titrating the point of equivalence between antigen and antibody and monitoring the point of equivalence by measuring the absorbance at 450nM as previously described (19). Neutrophils were stimulated as indicated and cultured in round bottom 96 well plates (Corning) in Dulbecco's PBS supplemented with Ca^{2+} and Mg^{2+}, 1g/L glucose and 4mM sodium bicarbonate in a humidified atmosphere at 37°C and 5% CO_2. After 6 hours, supernatants were harvested for cytokine analysis by ELISA (R&D research) according to manufacturer's instructions.

Statistical Analysis

For kinetic experiments, the area under the graph was used for analysis. Where data met the assumptions for parametric tests, two-tailed Student's *t*-tests were applied. Otherwise, the

non-parametric Mann-Whitney was test used. P-values <0.05 were considered statistically significant.

Results

Ptpn22$^{-/-}$ mice have already been described. In line with previous reports, we found them to be fertile and without overt deleterious or autoimmune phenotype (15, 26). *Ptpn22*$^{-/-}$ mice were characterized by mild peripheral blood neutrophilia (Fig 1A), complementing previous observations of increased B and T cell numbers in *Ptpn22*$^{-/-}$ mice (Hasegawa et al 2004, Maine et al 2015). To test whether this mild neutrophilia was a result of inadequate activation of *Ptpn22*$^{-/-}$ neutrophils, we analysed cell surface L-selectin / CD62L on freshly drawn peripheral blood neutrophils from control and *Ptpn22*$^{-/-}$ mice. This was similar, suggesting that the neutrophil activation status was not affected by the absence of PTPN22 (Fig 1B).

PTPN22 regulates neutrophil adhesion to immobilized immune complexes

Given the documented role of PTPN22, neutrophils and immune complexes (IC) in autoimmune driven inflammatory arthritis, we analysed IC-induced effector functions with purified, bone marrow derived neutrophils. When plating the cells onto surfaces that had been coated with immobilized ICs, fewer *Ptpn22*$^{-/-}$ than wild-type control neutrophils were found to adhere firmly (Fig 2A). In contrast, both *Ptpn22*$^{-/-}$ and wild-type (WT) control neutrophils were equally able to spread once attached to the immobilized ICs (Fig 2B,C). Similar results were obtained with neutrophils that had been allowed to bind to immobilized ICs for a shorter time (10 minutes; not shown). Neutrophils of both genotypes displayed very similar levels of surface FcγRII/III (Fig 2D). Since FcγRs and β2 integrins are known to cross-talk extensively (27, 28), we also characterised cell surface integrins. We observed no difference in cell surface expression of the common leukocyte β2 integrins LFA-1 / CD11a and noted a similar increase in cell surface Mac-1 / CD11b following stimulation of *Ptpn22*$^{-/-}$ and wild-type control neutrophils with fMLF (Fig 2D; supplemental Fig 1). These data suggest that reduced adhesion of *Ptpn22*$^{-/-}$ neutrophils was not due to reduced cell surface FcγR or integrin receptor density.

PTPN22 regulates adhesion- and FcγR-dependent ROS formation

FcγR engagement initiates specific neutrophil effector functions, including ROS production and degranulation. To test whether *Ptpn22*$^{-/-}$ neutrophils were able to generate ROS, we stimulated cells with the phorbol ester PMA (Fig 3A,B) or with a formylated peptide (fMLF) (Fig 3C,D). We noted no differences to control neutrophils. In contrast, ROS formation by *Ptpn22*$^{-/-}$ neutrophils that had been plated onto immobilized ICs was significantly lower than that seen with wild-type control neutrophils (Fig 3E,F). In-line with well-established cross-talk between FcγRs and integrins (27, 28), a similarly reduced generation of ROS was also observed when neutrophils were plated on the β2 integrin ligand fibrinogen in the presence of TNFα (Fig 3G,H) or onto the synthetic pan integrin ligand polyArgGlyAsp (Fig 3I,K). In conclusion, *Ptpn22*$^{-/-}$ neutrophils were characterized by reduced ROS production following FcγR and integrin-dependent stimulations.

PTPN22 regulates FcγR-dependent neutrophil degranulation

We next tested the ability of *Ptpn22*$^{-/-}$ neutrophils to degranulate by measuring the release of lactoferrin and gelatinase, components of neutrophil secondary and tertiary granules, respectively. As observed with ROS production, *Ptpn22*$^{-/-}$ neutrophils degranulated less efficiently than controls when plated onto immobilized ICs, but not when they were stimulated with fMLF in the presence of cytochalasin B (Fig 4 A-C). These data argue that PTPN22 is required for optimal neutrophil effector functions involved in generating an inflammatory environment following stimulation of FcγR (and integrins), and likely functioning in intracellular signaling events downstream of receptor engagement.

To address whether PTPN22 may also be involved in cytokine production, we analysed release of TNFα, MIP2 (a murine equivalent of IL-8) and IL-1β by neutrophils that had been stimulated with immune complexes. The extent of cytokine release triggered by IC-stimulation of neutrophils detected in these assays was very low and any reductions observed with *Ptpn22*$^{-/-}$ neutrophils did not reach significance (Supplemental Fig 2).

PTPN22 functions to activate signaling processes downstream of FcγRs

PTPN22 is a protein tyrosine phosphatase. Signaling downstream of FcγRs (and integrins) involves significant tyrosine phosphorylation. Receptor-proximal key signaling proteins regulated include the major neutrophil SFKs Lyn, Hck and Fgr, and the spleen tyrosine kinase (Syk). We analysed tyrosine phosphorylation of Syk immunoprecipitated from control and *Ptpn22*$^{-/-}$ lysates from neutrophils that had been plated onto immobilized ICs (IgG-BSA) or onto BSA (Fig 5A). Mock-stimulated *Ptpn22*$^{-/-}$ neutrophils were characterized by increased Syk tyrosine phosphorylation (221.4 ± 16.8% compared to control) as well as a second, slightly slower migrating band (indicated by * in Fig 5A) than wild-type controls. No differences were apparent between Syk tyrosine phosphorylation of activated wild-type and *Ptpn22*$^{-/-}$ neutrophils. Probing with an antibody that specifically recognises the activating phosphotyrosine residues Y519/Y520 in mouse Syk, revealed no differences between genotypes, with no signal in basal control or *Ptpn22*$^{-/-}$ neutrophils. This suggested that Syk tyrosine residue(s) other than Y519/Y520 are dephosphorylated either directly or indirectly by PTPN22 in the neutrophil.

Lyn has been shown to act as an inhibitory SFK that phosphorylates Syk in B cells (29, 30). We therefore analysed Lyn in control and *Ptpn22*$^{-/-}$ neutrophils. As a result of differential splicing Lyn is known to run as a doublet (31), however, at least with the antibody we employed, Lyn migrated as three distinct bands in basal and stimulated control cells as well as in basal *Ptpn22*$^{-/-}$ cells. In lysates from stimulated *Ptpn22*$^{-/-}$ neutrophils, we noticed a fourth Lyn band (Fig 5B, arrow). Given the short time-frame of the stimulation employed, this was likely caused by a post-translational modification of Lyn. We therefore immunoprecipitated Lyn for analysis with phosphorylation specific antibodies. This revealed increased total tyrosine phosphorylation of *Ptpn22*$^{-/-}$ neutrophils (150.1 ± 6.2% compared to control), and slight increases for both the activating Y527 residue (124.5 ± 6.1%), and the inhibitory Y416 residue (118 ± 2.7%). In addition, phosphorylated Lyn from *Ptpn22*$^{-/-}$ neutrophils migrated slower than Lyn from controls. This was particularly apparent for the

phospho-Y527 (Fig 5B, arrows). Taken together, our observations suggested that PTPN22 regulates Lyn phosphorylation in the neutrophil.

To further address the implications of PTPN22-mediated dephosphorylation events, we also analyzed the activity status of some key signaling intermediates that are activated downstream of SFK / Syk signaling following activation of FcγRs. We probed for phospho-PKB (also known as Akt), a read-out for the activity status of phosphoinositide 3-kinase, phospho-extracellular signal regulated kinase (Erk), and phospho-p38 mitogen activated protein (MAP) kinase. All of these signaling intermediates were found to be mildly hypophosphorylated in *Ptpn22*$^{-/-}$ neutrophils (Fig 5C-F), indicating that many signaling events downstream of FcγR engagement are influenced by PTPN22 in the neutrophil. Finally, phosphotyrosine blots of lysates from control and *Ptpn22*$^{-/-}$ neutrophils that had been plated onto BSA or immobilized immune complexes showed reduced tyrosine phosphorylation in basal and activated *Ptpn22*$^{-/-}$ lysates (supplemental Fig 3). Together, these *in vitro* data suggested that PTPN22 phosphatase performs activating dephosphorylation events in the neutrophil.

Ptpn22$^{-/-}$ mice are protected from K/BxN serum transfer arthritis

Given the association of the human PTPN22 SNP, C1858T with rheumatoid arthritis, we tested whether the *in vitro* observations were relevant *in vivo*. K/BxN serum was administered to control and *Ptpn22*$^{-/-}$ mice to induce serum transfer arthritis. *Ptpn22*$^{-/-}$ mice were significantly protected from inflammatory joint disease compared to age- and sex-matched wild-type controls. This was independent of the sex of the recipient animals, and the trend was observed with various doses of arthritogenic serum (Fig 6 and table I). *Ptpn22*$^{-/-}$ mice were characterized by slower progression of the disease and also reduced overall severity (Fig 6A). The clinical observations in the *Ptpn22*$^{-/-}$ mice were confirmed in histological sections taken near the height of inflammation (on day 5) which showed a reduced inflammatory cell infiltrate and few joint erosions when compared to wild-type controls (Fig 6B). Very few neutrophils were apparent in ankle joint sections at this time-point. Therefore, neutrophil infiltration was further evaluated at an earlier time-point (day 2), when neutrophil influx was expected to be maximal. Neutrophils in joint sections were visualized by their distinct morphology and by Ly6G staining (Fig 6C, red arrows). In contrast to controls and in keeping with the milder clinical disease, very few neutrophils were apparent in ankle joints of *Ptpn22*$^{-/-}$ mice.

PTPN22 does not regulate neutrophil migration or recruitment

Neutrophils have been shown to organise their own recruitment to the inflamed joint in K/BxN serum transfer arthritis. This is regulated by a series of chemokines and cytokines released by neutrophils and other synovial cells, that mediate recruitment of consecutive waves of neutrophils to the inflamed joint (32, 33). Since neutrophil migration into the inflamed joint is an absolute requirement for the generation of inflammation in this model (12–14), we analysed chemotaxis of *Ptpn22*$^{-/-}$ and control neutrophils. We observed no differences in terms of Euclidian or total accumulated distances travelled or indeed in the chemotactic directionality (the ratio between the Euclidian and the total accumulated distance) in Dunn chamber chemotaxis towards MIP-2, indicating that *Ptpn22*$^{-/-}$ neutrophils

undergo normal chemotaxis (Fig 7A-D). We further addressed whether the absence of PTPN22 might affect transendothelial migration (TEM), a key step required to enable neutrophils to leave the blood stream. TEM was assessed using an *in vitro* transwell chemotaxis assay, where neutrophils migrated through a transwell membrane supporting a monolayer of TNFα-stimulated murine endothelial cells. *Ptpn22*$^{-/-}$ deficient neutrophils migrated through these activated endothelial cells as efficiently as wild-type controls (Fig 7E), suggesting that PTPN22 does not regulate neutrophil TEM either. Finally, to test more definitively leukocyte recruitment *in vivo* we utilized the thioglycollate-induced sterile peritonitis model. Leukocyte recruitment was analysed at an early timepoint after induction of peritonitis, when neutrophil recruitment peaks ahead of the recruitment of other leukocytes (34). Again, and in line with the *in vitro* observations above, there was no detectable defect in neutrophil recruitment to the inflamed peritoneum of *Ptpn22*$^{-/-}$ deficient mice (Fig 7F). These observations demonstrate that PTPN22 does not regulate neutrophil chemotaxis, TEM or recruitment per se. Rather, PTPN22 influences the activation of neutrophils in response to ICs.

Discussion

Our data show a significant protection of *Ptpn22*$^{-/-}$ mice from immune complex-driven K/BxN serum transfer arthritis. This model tests the effector phase of arthritis, which depends on neutrophil activation for its clinical expression. Protection was observed with both males and females under a number of experimental conditions (Fig 6 and Table I). In contrast to our results, Wang et al (35) and Maine et al (36) noted no protection from joint protection using the K/BxN model in *Ptpn22*$^{-/-}$ mice. We suspect that these discrepancies may be the result of differences in the experimental conditions. Both studies induced arthritis by injecting larger amounts of arthritogenic serum than ourselves, inducing a severe and prolonged arthritis. In contrast, we aimed for sub-maximal transient arthritis, that would enable the detection of subtle differences between experimental cohorts. It is conceivable that the degree of neutrophil stimulation induced in these studies overrode the protection afforded by the lack of PTPN22. In addition, it is possible that differences in housing conditions would lead to variations in the microbiome of the mice used for the different studies. The gastrointestinal microbiota has recently been recognized to regulate immunity and inflammatory responses to *in vivo* challenges (37). Interestingly, K/BxN arthritis depends heavily on the microbiome, with the T cell independent effector phase of K/BxN serum transfer arthritis being regulated by gut microbiota (38, 39).

In vitro, with *Ptpn22*$^{-/-}$ neutrophils, we observed normal chemotaxis and transendothelial migration towards MIP2. *In vivo,* normal levels of neutrophil recruitment in the thioglycollate induced model of peritonitis was also apparent in *Ptpn22*$^{-/-}$ mice. This argues against a role for PTPN22 in neutrophil migration or recruitment (Fig 7). In contrast, few neutrophils were observed in the ankle joints of *Ptpn22*$^{-/-}$ mice following the induction of K/BxN arthritis (Fig 6). One explanation for this difference is that alternative mechanisms may be utilized by neutrophils migrating to different sites. Neutrophils have been shown to promote their own recruitment to inflamed joints in the K/BxN serum transfer arthritis model, by generating chemokines and inciting other cells to do the same (32, 33). Therefore, an alternative explanation maybe that *Ptpn22*$^{-/-}$ neutrophils were less efficient at promoting a

suitable inflammatory environment to drive forward further waves of neutrophil recruitment, as seen with the K/BxN serum transfer arthritis. *In vitro*, neutrophil activation by immobilized ICs was defective, whilst stimulation induced by fMLF or PMA was not (Fig 3, 4). This indicates that PTPN22 is likely to be preferentially involved in inflammation, induced following integrin and/or Fcγ R-dependent neutrophil activation.

Our observations are reminiscent of recent reports with Syk and SFK triple knock-out neutrophils, that provided complete protection from K/BxN serum transfer arthritis (40, 41). In these reports, Syk along with Lyn, Hck and Fgr were shown to be dispensable for neutrophil recruitment. Yet they played a crucial role in Fcγ R / integrin mediated neutrophil effector functions, including the generation of chemokines, that are required to generation inflammation (40, 41). We analysed IC induced chemokine generation by *Ptpn22*$^{-/-}$ neutrophils (Supplemental Fig 2). Overall cytokine secretion in these experiments was low and any differences between genotypes did not reach significance. It is likely such differences will be more pronounced with inflammatory neutrophils, such as those within the synovial fluid of the arthritic joint, than with unprimed, bone marrow derived neutrophils. It will be interesting to address these issues in more depth in the future.

Interestingly, our data suggest that both Lyn and Syk tyrosine phosphorylation are affected in *Ptpn22*$^{-/-}$ neutrophils (Fig 5). We do not yet know the identity of the affected phosphorylation sites, nor whether these were direct events. It will be interesting to identify the exact nature of neutrophil PTPN22 substrates in the future. Given that the protection from K/BxN serum transfer arthritis afforded by *Ptpn22*$^{-/-}$ mice was larger than that of any individual SFK (Hck, Fgr or Lyn) (41), it is interesting to speculate that PTPN22 may contribute to regulating several SFKs, as well as other potential substrates. Such a function would be in keeping with our current understanding of PTPN22 function in T cells, where PTPN22 has been shown to dephosphorylate tyrosine residues within the SFKs Lck and Fyn; ZAP-70, a Syk family protein and also immune receptor tyrosine based activation motifs (ITAMS) in TCR associated proteins (26, 42, 43). Whilst these substrates are not expressed in neutrophils, some of their family members are.

The findings presented here contrast sharply with observations by others who analyzed the role of PTPN22 in lymphocytes. In T cells, PTPN22 functions as a negative regulator (44). For instance, T cell receptor signaling and cell adhesion, mediated by Rap dependent integrin inside-out signaling were increased in *Ptpn22*$^{-/-}$ mice (15). The activating role of PTPN22 downstream of Fcγ Rs might be specific to the neutrophil, suggesting that PTPN22 expression might individually modulate various leukocytes that contribute to inflammation.

A missense SNP in PTPN22 (PTPN22-C1858T) predisposes carriers to a number of autoimmune diseases, most notably RA, SLE and type 1 diabetes (43, 45, 46). However, it protects against Behcets disease and bowel inflammation secondary to Crohn’s disease. Both of these diseases are characterized by significant neutrophil mediated chronic inflammation (47, 48). Our understanding of PTPN22 function and biochemistry, in particular in the neutrophil, lags behind studies of its function in T cells. Indeed, the effects of the R620W mutation is still being debated, with suggestions varying between the mutation being activating, inactivating and a hypomorph (45). Moreover, observations in the mouse do not

always tally with those in humans, with studies in human cells split between those suggesting the R620W variant is a gain of function (43, 49), and others suggesting that it is a loss of function (50). In contrast, most studies conducted in the mouse are more suggestive of a loss of function mutation (51, 52). Furthermore, genetic background, as well as the presence of other, potentially as yet unidentified susceptibility alleles may play a role. R619W *Ptpn22* knock-ins largely replicated the phenotype of *Ptpn22*$^{-/-}$ lymphocytes, suggestive of a loss of function mutation. One study suggested R619W PTPN22 is prone to degradation (52). However in a separately derived knock-in, protein stability was not impaired and mice kept on a mixed 129 x C57Bl/6 background, which is more prone to autoimmunity than pure C57Bl/6 developed mild, spontaneous autoimmune disease (51).

In ascribing to PTPN22 an activating function, our work is suggestive, at least in the neutrophil, of a gain of function with R620W PTPN22. In the context of the results described here, it is hard to explain how a loss of function mutation would trigger enhanced inflammation in immune receptor dependent contexts, such as the K/BxN model for arthritis. It will be very interesting to test this hypothesis in the future by analyzing neutrophils derived from a R619W *Ptpn22* point mutation knock-in mouse. As noted above, such mice have already been generated, but their analysis to date has been restricted to cell types outwith the neutrophil (51, 52). One recent study analyzed effector functions in human neutrophils derived from healthy donors and from RA patients that were or were not homozygous carriers of the SNP (53). Whilst that study did not test any IC-dependent events, the authors reported that neutrophils from homozygous carriers generate increased ROS, release more calcium in response to other stimulations and undergo faster transendothelial migration than those from matched control donors, in general agreement with the notion that R620W PTPN22 acts as a gain of function mutation in neutrophils.

Supplementary Material

Refer to Web version on PubMed Central for supplementary material.

Acknowledgements

We thank Adriano Rossi, Ian Dransfield and Moira Whyte for helpful discussions, Nick Ktistakis for antibodies and Kev Dhaliwal for access to equipment.

Work in MG's laboratory was supported by the Arthritis-Research-UK [20035] and the Medical Research Council [MR/J009555/1]. Work in SV's laboratory was supported by a University of Edinburgh Chancellor's Fellowship and a Wellcome Trust ISSF award.

References

1. Quayle JA, Watson F, Bucknall RC, Edwards SW. Neutrophils from the synovial fluid of patients with rheumatoid arthritis express the high affinity immunoglobulin G receptor, Fc gamma RI (CD64): role of immune complexes and cytokines in induction of receptor expression. Immunology. 1997; 91:266–273. [PubMed: 9227327]
2. Robinson JJ, Watson F, Bucknall RC, Edwards SW. Role of Fc gamma receptors in the activation of neutrophils by soluble and insoluble immunoglobulin aggregates isolated from the synovial fluid of patients with rheumatoid arthritis. Annals of the rheumatic diseases. 1994; 53:515–520. [PubMed: 7944636]

3. Nathan C. Neutrophils and immunity: challenges and opportunities. Nature reviews Immunology. 2006; 6:173–182.
4. Wright HL, Moots RJ, Edwards SW. The multifactorial role of neutrophils in rheumatoid arthritis. Nature reviews Rheumatology. 2014; 10:593–601. [PubMed: 24914698]
5. Viatte S, Plant D, Raychaudhuri S. Genetics and epigenetics of rheumatoid arthritis. Nature reviews Rheumatology. 2013; 9:141–153. [PubMed: 23381558]
6. Hinks A, Cobb J, Marion MC, Prahalad S, Sudman M, Bowes J, Martin P, Comeau ME, Sajuthi S, Andrews R, Brown M, et al. Dense genotyping of immune-related disease regions identifies 14 new susceptibility loci for juvenile idiopathic arthritis. Nature genetics. 2013; 45:664–669. [PubMed: 23603761]
7. Chien W, Tidow N, Williamson EA, Shih LY, Krug U, Kettenbach A, Fermin AC, Roifman CM, Koeffler HP. Characterization of a myeloid tyrosine phosphatase, Lyp, and its role in the Bcr-Abl signal transduction pathway. The Journal of biological chemistry. 2003; 278:27413–27420. [PubMed: 12764153]
8. Cloutier JF, Veillette A. Association of inhibitory tyrosine protein kinase p50csk with protein tyrosine phosphatase PEP in T cells and other hemopoietic cells. The EMBO journal. 1996; 15:4909–4918. [PubMed: 8890164]
9. Gregorieff A, Cloutier JF, Veillette A. Sequence requirements for association of protein-tyrosine phosphatase PEP with the Src homology 3 domain of inhibitory tyrosine protein kinase p50(csk). The Journal of biological chemistry. 1998; 273:13217–13222. [PubMed: 9582365]
10. Korganow AS, Ji H, Mangialaio S, Duchatelle V, Pelanda R, Martin T, Degott C, Kikutani H, Rajewsky K, Pasquali JL, Benoist C, et al. From systemic T cell self-reactivity to organ-specific autoimmune disease via immunoglobulins. Immunity. 1999; 10:451–461. [PubMed: 10229188]
11. Kouskoff V, Korganow AS, Duchatelle V, Degott C, Benoist C, Mathis D. Organ-specific disease provoked by systemic autoimmunity. Cell. 1996; 87:811–822. [PubMed: 8945509]
12. Monach PA, Nigrovic PA, Chen M, Hock H, Lee DM, Benoist C, Mathis D. Neutrophils in a mouse model of autoantibody-mediated arthritis: critical producers of Fc receptor gamma, the receptor for C5a, and lymphocyte function-associated antigen 1. Arthritis and rheumatism. 2010; 62:753–764. [PubMed: 20191628]
13. Wipke BT, Allen PM. Essential role of neutrophils in the initiation and progression of a murine model of rheumatoid arthritis. Journal of immunology. 2001; 167:1601–1608.
14. Kim ND, Chou RC, Seung E, Tager AM, Luster AD. A unique requirement for the leukotriene B4 receptor BLT1 for neutrophil recruitment in inflammatory arthritis. The Journal of experimental medicine. 2006; 203:829–835. [PubMed: 16567386]
15. Brownlie RJ, Miosge LA, Vassilakos D, Svensson LM, Cope A, Zamoyska R. Lack of the phosphatase PTPN22 increases adhesion of murine regulatory T cells to improve their immunosuppressive function. Science signaling. 2012; 5:ra87. [PubMed: 23193160]
16. Gray M, Miles K, Salter D, Gray D, Savill J. Apoptotic cells protect mice from autoimmune inflammation by the induction of regulatory B cells. Proceedings of the National Academy of Sciences of the United States of America. 2007; 104:14080–14085. [PubMed: 17715067]
17. Ellson CD, Davidson K, Ferguson GJ, O'Connor R, Stephens LR, Hawkins PT. Neutrophils from p40phox-/- mice exhibit severe defects in NADPH oxidase regulation and oxidant-dependent bacterial killing. The Journal of experimental medicine. 2006; 203:1927–1937. [PubMed: 16880254]
18. Ferguson GJ, Milne L, Kulkarni S, Sasaki T, Walker S, Andrews S, Crabbe T, Finan P, Jones G, Jackson S, Camps M, et al. PI(3)Kgamma has an important context-dependent role in neutrophil chemokinesis. Nature cell biology. 2007; 9:86–91. [PubMed: 17173040]
19. Fossati G, Bucknall RC, Edwards SW. Insoluble and soluble immune complexes activate neutrophils by distinct activation mechanisms: changes in functional responses induced by priming with cytokines. Annals of the rheumatic diseases. 2002; 61:13–19. [PubMed: 11779751]
20. Gambardella L, Anderson KE, Jakus Z, Kovacs M, Voigt S, Hawkins PT, Stephens L, Mocsai A, Vermeren S. Phosphoinositide 3-OH kinase regulates integrin-dependent processes in neutrophils by signaling through its effector ARAP3. Journal of immunology. 2013; 190:381–391.

21. Zicha D, Dunn GA, Brown AF. A new direct-viewing chemotaxis chamber. Journal of cell science. 1991; 99(Pt 4):769–775. [PubMed: 1770004]
22. Bixel MG, Li H, Petri B, Khandoga AG, Khandoga A, Zarbock A, Wolburg-Buchholz K, Wolburg H, Sorokin L, Zeuschner D, Maerz S, et al. CD99 and CD99L2 act at the same site as, but independently of, PECAM-1 during leukocyte diapedesis. Blood. 2010; 116:1172–1184. [PubMed: 20479283]
23. Mocsai A, Ligeti E, Lowell CA, Berton G. Adhesion-dependent degranulation of neutrophils requires the Src family kinases Fgr and Hck. Journal of immunology. 1999; 162:1120–1126.
24. Abdel-Latif D, Steward M, Macdonald DL, Francis GA, Dinauer MC, Lacy P. Rac2 is critical for neutrophil primary granule exocytosis. Blood. 2004; 104:832–839. [PubMed: 15073033]
25. Gambardella L, Anderson KE, Nussbaum C, Segonds-Pichon A, Margarido T, Norton L, Ludwig T, Sperandio M, Hawkins PT, Stephens L, Vermeren S. The GTPase-activating protein ARAP3 regulates chemotaxis and adhesion-dependent processes in neutrophils. Blood. 2011; 118:1087–1098. [PubMed: 21490342]
26. Hasegawa K, Martin F, Huang G, Tumas D, Diehl L, Chan AC. PEST domain-enriched tyrosine phosphatase (PEP) regulation of effector/memory T cells. Science. 2004; 303:685–689. [PubMed: 14752163]
27. Mocsai A, Abram CL, Jakus Z, Hu Y, Lanier LL, Lowell CA. Integrin signaling in neutrophils and macrophages uses adaptors containing immunoreceptor tyrosine-based activation motifs. Nature immunology. 2006; 7:1326–1333. [PubMed: 17086186]
28. Abram CL, Lowell CA. Convergence of immunoreceptor and integrin signaling. Immunological reviews. 2007; 218:29–44. [PubMed: 17624942]
29. Keshvara LM, Isaacson CC, Yankee TM, Sarac R, Harrison ML, Geahlen RL. Syk- and Lyn-dependent phosphorylation of Syk on multiple tyrosines following B cell activation includes a site that negatively regulates signaling. Journal of immunology. 1998; 161:5276–5283.
30. Pereira S, Lowell C. The Lyn tyrosine kinase negatively regulates neutrophil integrin signaling. Journal of immunology. 2003; 171:1319–1327.
31. Yi TL, Bolen JB, Ihle JN. Hematopoietic cells express two forms of lyn kinase differing by 21 amino acids in the amino terminus. Mol Cell Biol. 1991; 11:2391–2398. [PubMed: 2017160]
32. Chou RC, Kim ND, Sadik CD, Seung E, Lan Y, Byrne MH, Haribabu B, Iwakura Y, Luster AD. Lipid-cytokine-chemokine cascade drives neutrophil recruitment in a murine model of inflammatory arthritis. Immunity. 2010; 33:266–278. [PubMed: 20727790]
33. Sadik CD, Kim ND, Iwakura Y, Luster AD. Neutrophils orchestrate their own recruitment in murine arthritis through C5aR and FcgammaR signaling. Proceedings of the National Academy of Sciences of the United States of America. 2012; 109:E3177–3185. [PubMed: 23112187]
34. Pan D, Amison RT, Riffo-Vasquez Y, Spina D, Cleary SJ, Wakelam MJ, Page CP, Pitchford SC, Welch HC. P-Rex and Vav Rac-GEFs in platelets control leukocyte recruitment to sites of inflammation. Blood. 2015; 125:1146–1158. [PubMed: 25538043]
35. Wang Y, Shaked I, Stanford SM, Zhou W, Curtsinger JM, Mikulski Z, Shaheen ZR, Cheng G, Sawatzke K, Campbell AM, Auger JL, et al. The autoimmunity-associated gene PTPN22 potentiates toll-like receptor-driven, type 1 interferon-dependent immunity. Immunity. 2013; 39:111–122. [PubMed: 23871208]
36. Maine CJ, Marquardt K, Cheung J, Sherman LA. PTPN22 controls the germinal center by influencing the numbers and activity of T follicular helper cells. Journal of immunology. 2014; 192:1415–1424.
37. Kamada N, Seo SU, Chen GY, Nunez G. Role of the gut microbiota in immunity and inflammatory disease. Nature reviews Immunology. 2013; 13:321–335.
38. Wu HJ, Ivanov II, Darce J, Hattori K, Shima T, Umesaki Y, Littman DR, Benoist C, Mathis D. Gut-residing segmented filamentous bacteria drive autoimmune arthritis via T helper 17 cells. Immunity. 2010; 32:815–827. [PubMed: 20620945]
39. Lee H, Jin BE, Jang E, Lee AR, Han DS, Kim HY, Youn J. Gut-residing Microbes Alter the Host Susceptibility to Autoantibody-mediated Arthritis. Immune Netw. 2014; 14:38–44. [PubMed: 24605079]

40. Elliott ER, Van Ziffle JA, Scapini P, Sullivan BM, Locksley RM, Lowell CA. Deletion of Syk in neutrophils prevents immune complex arthritis. Journal of immunology. 2011; 187:4319–4330.
41. Kovacs M, Nemeth T, Jakus Z, Sitaru C, Simon E, Futosi K, Botz B, Helyes Z, Lowell CA, Mocsai A. The Src family kinases Hck, Fgr, and Lyn are critical for the generation of the in vivo inflammatory environment without a direct role in leukocyte recruitment. The Journal of experimental medicine. 2014; 211:1993–2011. [PubMed: 25225462]
42. Stanford SM, Krishnamurthy D, Falk MD, Messina R, Debnath B, Li S, Liu T, Kazemi R, Dahl R, He Y, Yu X, et al. Discovery of a novel series of inhibitors of lymphoid tyrosine phosphatase with activity in human T cells. Journal of medicinal chemistry. 2011; 54:1640–1654. [PubMed: 21341673]
43. Vang T, Liu WH, Delacroix L, Wu S, Vasile S, Dahl R, Yang L, Musumeci L, Francis D, Landskron J, Tasken K, et al. LYP inhibits T-cell activation when dissociated from CSK. Nature chemical biology. 2012; 8:437–446. [PubMed: 22426112]
44. Zheng J, Petersen F, Yu X. The role of PTPN22 in autoimmunity: learning from mice. Autoimmunity reviews. 2014; 13:266–271. [PubMed: 24189282]
45. Bottini N, Peterson EJ. Tyrosine phosphatase PTPN22: multifunctional regulator of immune signaling, development, and disease. Annu Rev Immunol. 2014; 32:83–119. [PubMed: 24364806]
46. International Consortium for Systemic Lupus Erythematosus, G. Harley JB, Alarcon-Riquelme ME, Criswell LA, Jacob CO, Kimberly RP, Moser KL, Tsao BP, Vyse TJ, Langefeld CD, Nath SK, et al. Genome-wide association scan in women with systemic lupus erythematosus identifies susceptibility variants in ITGAM, PXK, KIAA1542 and other loci. Nature genetics. 2008; 40:204–210. [PubMed: 18204446]
47. Baranathan V, Stanford MR, Vaughan RW, Kondeatis E, Graham E, Fortune F, Madanat W, Kanawati C, Ghabra M, Murray PI, Wallace GR. The association of the PTPN22 620W polymorphism with Behcet's disease. Annals of the rheumatic diseases. 2007; 66:1531–1533. [PubMed: 17660222]
48. Barrett JC, Hansoul S, Nicolae DL, Cho JH, Duerr RH, Rioux JD, Brant SR, Silverberg MS, Taylor KD, Barmada MM, Bitton A, et al. Genome-wide association defines more than 30 distinct susceptibility loci for Crohn's disease. Nature genetics. 2008; 40:955–962. [PubMed: 18587394]
49. Vang T, Congia M, Macis MD, Musumeci L, Orru V, Zavattari P, Nika K, Tautz L, Tasken K, Cucca F, Mustelin T, et al. Autoimmune-associated lymphoid tyrosine phosphatase is a gain-of-function variant. Nature genetics. 2005; 37:1317–1319. [PubMed: 16273109]
50. Zikherman J, Hermiston M, Steiner D, Hasegawa K, Chan A, Weiss A. PTPN22 deficiency cooperates with the CD45 E613R allele to break tolerance on a non-autoimmune background. Journal of immunology. 2009; 182:4093–4106.
51. Dai X, James RG, Habib T, Singh S, Jackson S, Khim S, Moon RT, Liggitt D, Wolf-Yadlin A, Buckner JH, Rawlings DJ. A disease-associated PTPN22 variant promotes systemic autoimmunity in murine models. The Journal of clinical investigation. 2013; 123:2024–2036. [PubMed: 23619366]
52. Zhang J, Zahir N, Jiang Q, Miliotis H, Heyraud S, Meng X, Dong B, Xie G, Qiu F, Hao Z, McCulloch CA, et al. The autoimmune disease-associated PTPN22 variant promotes calpain-mediated Lyp/Pep degradation associated with lymphocyte and dendritic cell hyperresponsiveness. Nature genetics. 2011; 43:902–907. [PubMed: 21841778]
53. Bayley R, Kite KA, McGettrick HM, Smith JP, Kitas GD, Buckley CD, Young SP. The autoimmune-associated genetic variant PTPN22 R620W enhances neutrophil activation and function in patients with rheumatoid arthritis and healthy individuals. Annals of the rheumatic diseases. 2014

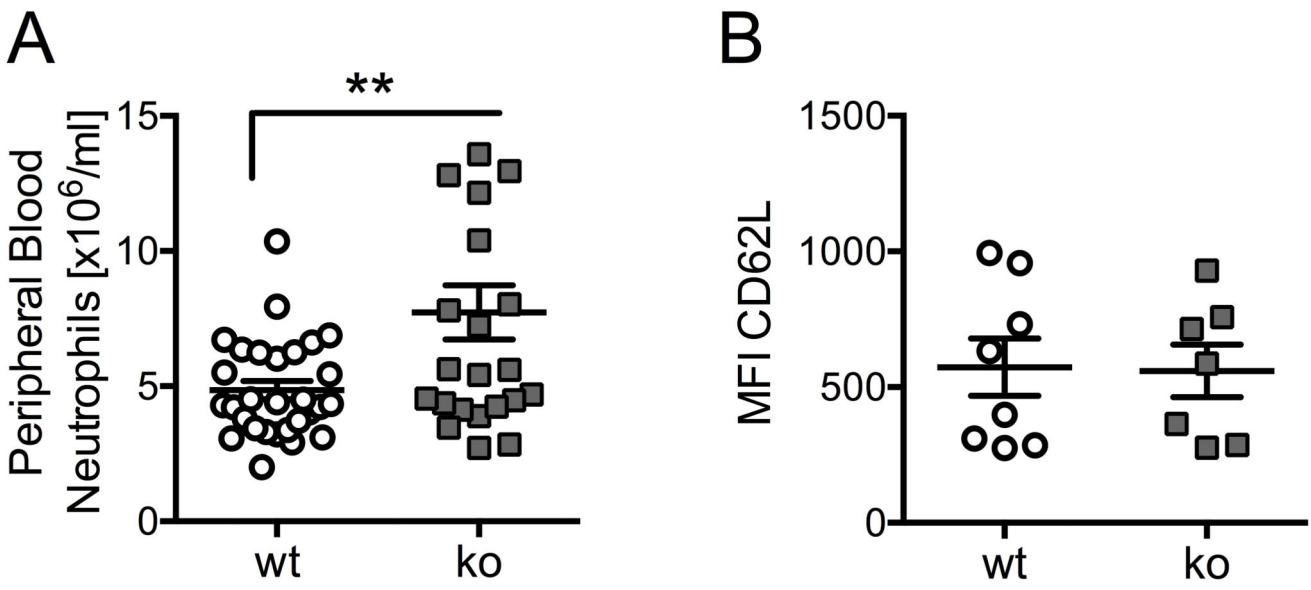

Figure 1. *Ptpn22*$^{-/-}$ mice have mild neutrophilia.

(A) *Ptpn22*$^{-/-}$ mice have mild neutrophilia. Bloods from 17 *Ptpn22*$^{-/-}$ and 22 matched control mice were labeled for CD11b and Ly6G and analysed by flow cytometry. Data (means ± SEM) were pooled from four separate experiments; **, $p<0.01$. (B) Cell surface L-selectin was analysed in unstimulated neutrophils from bloods of 8 wild-type and 7 *Ptpn22*$^{-/-}$ mice. Neutrophils were gated for analysis of CD62L staining; MFIs are plotted.

Europe PMC Funders Author Manuscripts

Europe PMC Funders Author Manuscripts

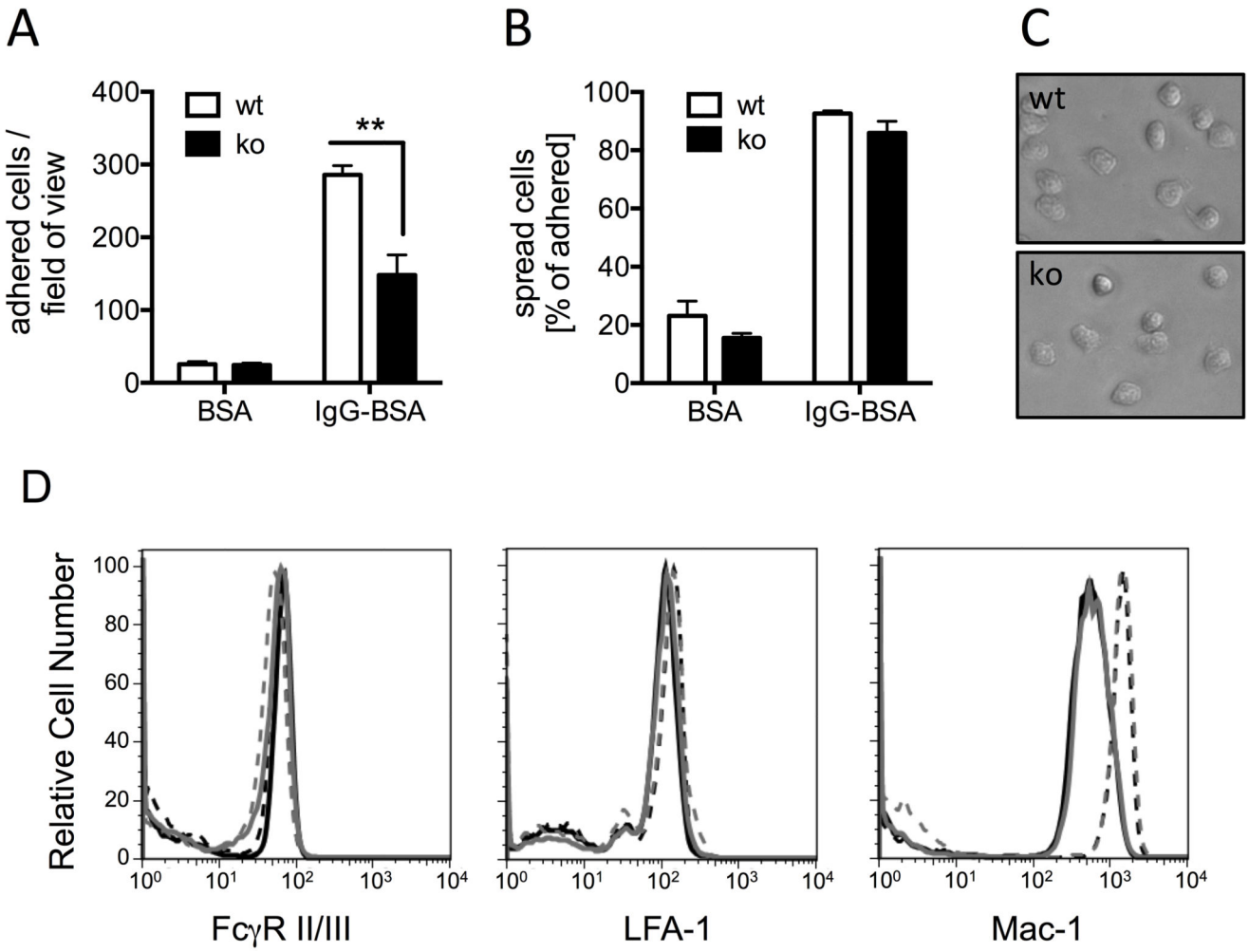

Figure 2. *Ptpn22*$^{-/-}$ mice have a defect in adhering to immobilized ICs.

Neutrophils isolated from bone marrows of *Ptpn22*$^{-/-}$ (ko) and matched wild-type control (wt) mice were allowed to adhere for 20 minutes to wells that had been coated with immobilized ICs (IgG-BSA) or BSA as control, followed by washing and fixing. Adherent and spread cells were counted in four randomly photographed fields of view of each well. (A) Total number of all adhered cells. (B) Percentage of spread cells out of total. (A,B) Pooled data (means ± SEM) from three separate experiments are presented; **, $p < 0.01$. (C) Representative examples of *Ptpn22*$^{-/-}$ and matched control neutrophils allowed to adhere to immobilized ICs for 20 minutes. (D) Surface FcγRII/III, LFA-1 and Mac-1 of purified bone marrow derived neutrophils from control and *Ptpn22*$^{-/-}$ mice were analyzed by flow cytometry. Neutrophils were or were not stimulated with fMLF at 37°C before being labelled with FITC-conjugated anti-GR1 and PE-conjugated anti-FcγRII/III, anti-Mac1 or anti-LFA1. GR1 positive cells were gated and PE staining was measured. Results were analysed using FlowJo software. Black lines, wild-type neutrophils; grey lines, *Ptpn22*$^{-/-}$ neutrophils. Full lines, unstimulated cells and broken lines, stimulated cells. Experiments were performed with cells from four animals / genotype and representative examples are shown. Please see supplemental Fig 1 for a graphical representation of all experiments.

Europe PMC Funders Author Manuscripts

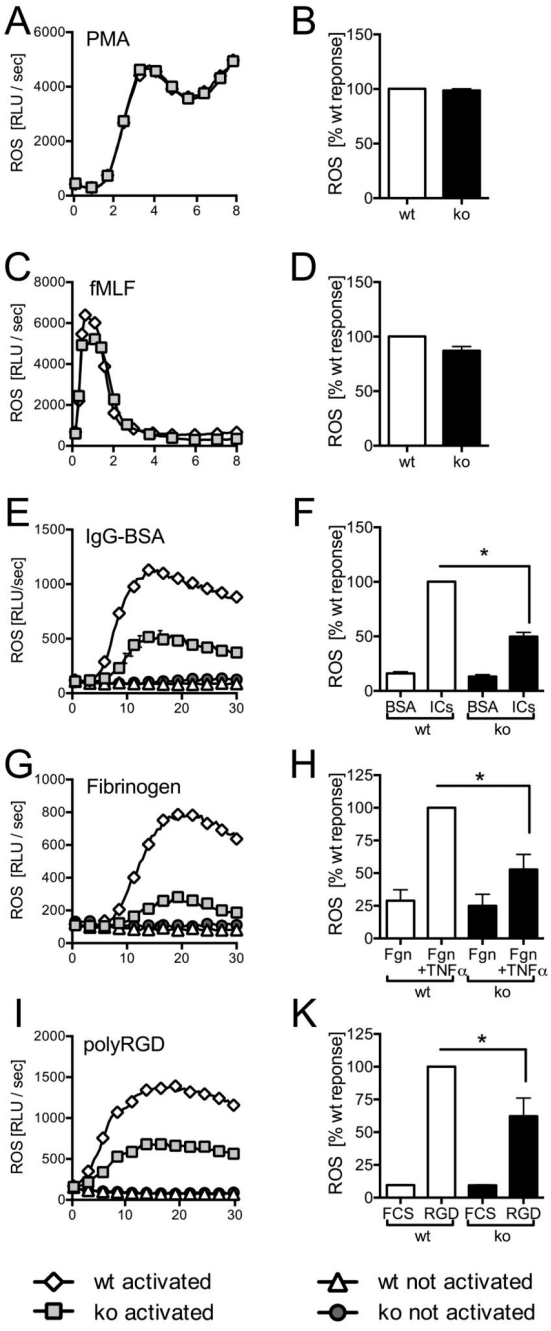

Figure 3. *Ptpn22*$^{-/-}$ neutrophils are characterized by impaired immune receptor induced ROS production.

Neutrophils isolated from bone marrows of *Ptpn22*$^{-/-}$ (ko) and matched wild-type control (wt) mice were used to characterize ROS production following stimulation with PMA (A,B), with fMLF (C,D), or following plating of cells into wells coated with immobilized IC (IgG-BSA) or as a control, BSA (E,F), into fibrinogen coated wells in the presence (stimulated) of absence (control) of TNFα (G, H), or into wells coated with the synthetic integrin ligand poly-Arg-Gly-Asp (polyRGD) or as a control, heat inactivated fetal calf serum (FCS) (I,K). Data shown (means ± range) are representative individual experiments (A,C,E,G,I). Total

light emissions (means ± SEM) expressed as percentage of the response obtained with stimulated control neutrophils pooled from a minimum of three separate experiments (B,D,F,H,K).

Europe PMC Funders Author Manuscripts

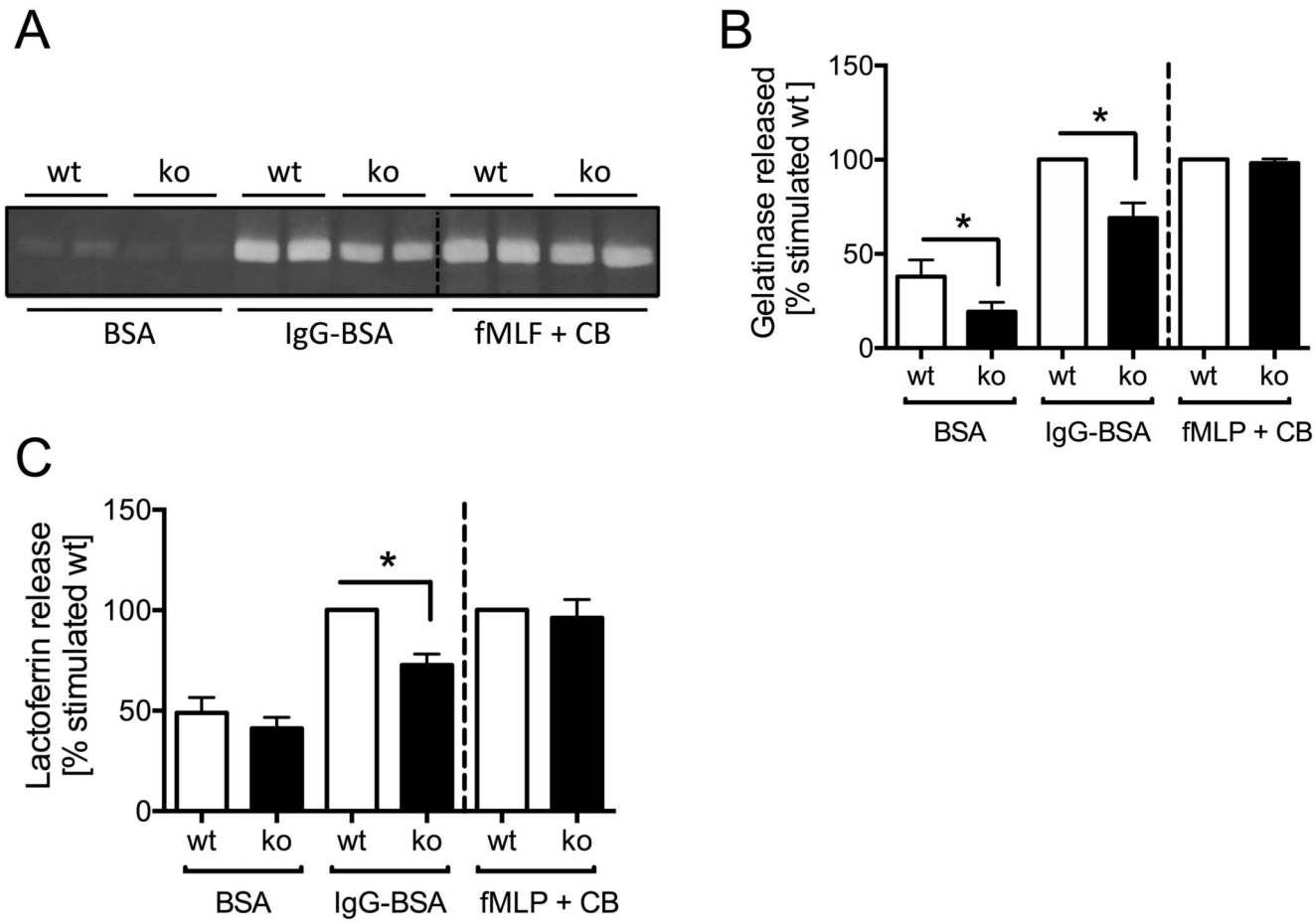

Figure 4. *Ptpn22*$^{-/-}$ neutrophils are characterized by reduced immune complex induced degranulation.

(A,B) Gelatinase release by control (wt) and *Ptpn22*$^{-/-}$ (ko) neutrophils plated into wells coated with immobilized ICs (IgG-BSA) or as a control, BSA, or that had been stimulated by fMLF in the presence of cytochalasin B (fMLF + CB) was assessed by in-gel zymography. A representative experiment (A) and pooled data (means ± SEM) from five separately performed experiments (B) are presented. (C) Lactoferrin release by control and *Ptpn22*$^{-/-}$ neutrophils plated into wells coated with immobilized ICs (IgG-BSA) or as a control, BSA, or that had been stimulated by fMLF in the presence of cytochalasin B (fMLF + CB) was assayed by ELISA. Pooled data from three separate experiments are presented. Data presented are normalized to activated wild-type.

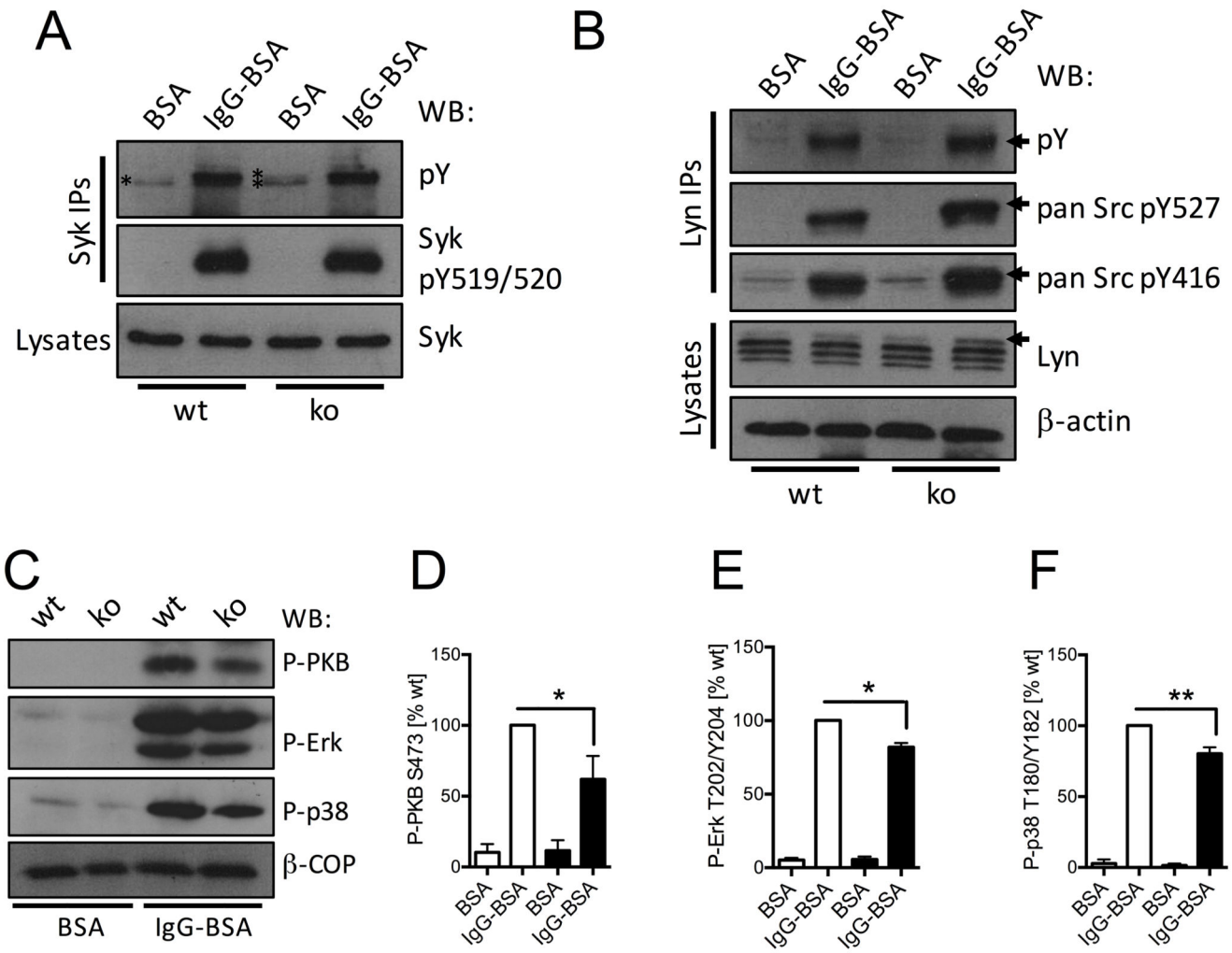

Figure 5. Neutrophil PTPN22 regulates Lyn and Syk tyrosine phosphorylation which affects the activity status of many signaling cascades.

Neutrophils isolated from bone marrows of *Ptpn22*$^{-/-}$ (ko) and matched wild-type control (wt) mice were allowed to adhere to immobilized ICs (IgG-BSA) or, as a control, BSA for 12 minutes. (A,B) Lysates were prepared as detailed in Materials and Methods for Western blotting using the indicated antibodies; in addition, Syk (A) or Lyn (B) were immunoprecipitated for analysis of phosphotyrosine as well as probing with antibodies detecting specific tyrosine phosphorylations in Syk / SFK proteins as indicated. Representative sample from at least 3 separately performed experiments are shown. (C-F) Lysates were prepared and subjected to immunoblotting with antibodies specific for phospho-PKB, phospho-Erk and phospho-p38 MAPK (C-F). Blots were quantitated using Image J software. (C) Representative blots; (D-F) Densitometry from five separate experiments (means ± SEM) was normalized to activated controls; *, $p<0.05$; **, $p<0.01$.

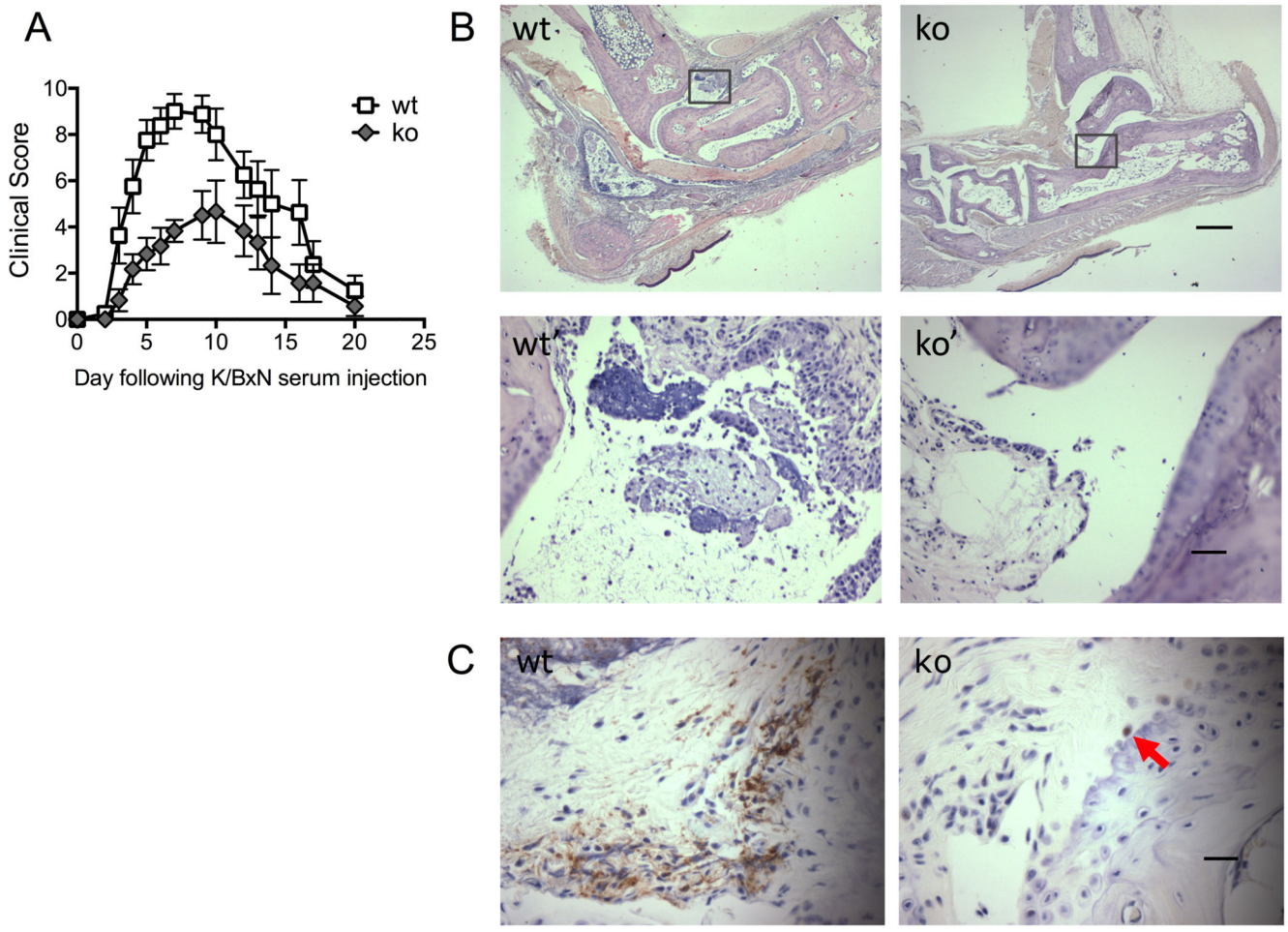

Figure 6. *Ptpn22*$^{-/-}$ mice are protected from K/BxN arthritis.

K/BxN serum transfer arthritis was induced in *Ptpn22*$^{-/-}$ (ko) and matched control (wt) mice. (A) Clinical scores (Means ± SEM) of the experimental groups were plotted over 20 days. Four experiments were carried out with 5-8 animals in each experimental group; a representative experiment is shown; experimental groups behaved significantly different, p = 0.02. (B) Wax sections of decalcified joints were H&E stained to visualize joint erosion and leukocyte infiltration on day 5 after serum transfer. Representative examples from sections obtained with right rear joints of arthritogenic serum injected control (wt) and *Ptpn22*$^{-/-}$ (ko) mice are shown (scale bar, 500μm); panels wt' and ko' are higher power images of the boxed areas in panels wt and ko (scale bar, 50μm). (C) Wax sections of decalcified joints were stained with an antibody specific for Ly6G and counterstained with hematoxylin to visualize neutrophil infiltration at day 2 following administration of arthritogenic serum. A red arrow in *Ptpn22*$^{-/-}$ points out a rare neutrophil (scale bar, 25μm).

Europe PMC Funders Author Manuscripts

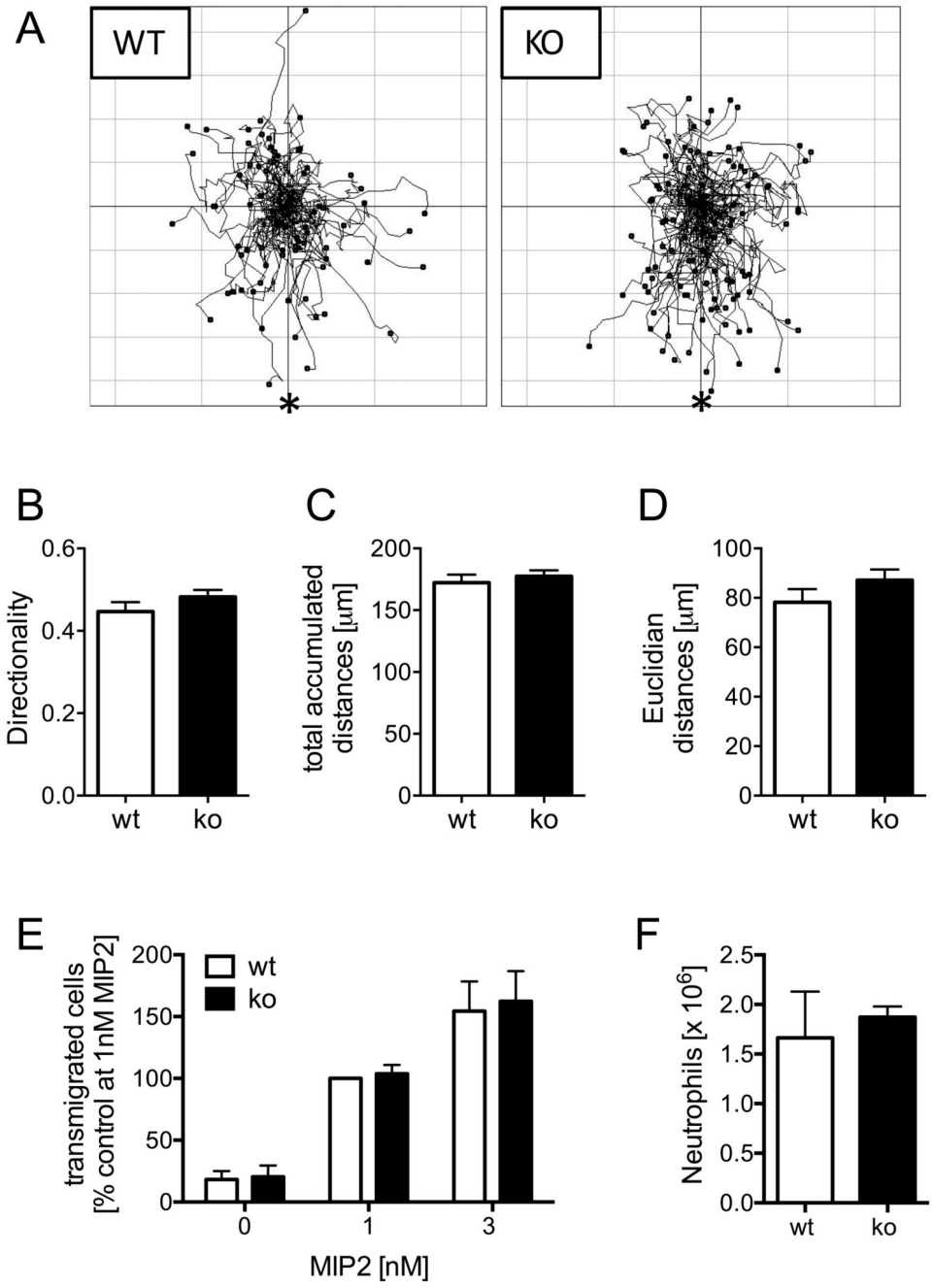

Figure 7. Neutrophil chemotaxis and recruitment are not affected in *Ptpn22*$^{-/-}$ mice.

(A-D) Neutrophils isolated from bone marrows of *Ptpn22*$^{-/-}$ (ko) and matched wild-type control (wt) mice were allowed to chemotax towards 10nM MIP2 in Dunn chambers. Cell migration was monitored by time-lapse imaging, and individual cells were tracked using a cell tracking plug-in into Image J. (A) Tracks obtained in experiments carried out with three separate preparations of bone marrow derived neutrophils analysed were pooled for these spider plots. The source of chemoattractant is indicated (*). (B-D) The coordinates for the tracks shown in (A) were analysed using statistics features of the Ibidi chemotaxis plug-in

into Image J as detailed in Materials and Methods. Parameters presented (means ± SEM) are, directionality (B), total accumulated (C) and Euclidian distances (D); differences were not statistically significant. (E) *Ptpn22*$^{-/-}$ (ko) and control (wt) neutrophils were allowed to migrate towards indicated concentrations of MIP2 in transwells supporting a monolayer of TNFα stimulated mouse endothelial cells. Data (means ± SEM) expressed as percentage of control cells migrating towards 1nM MIP2 from two pooled experiments carried out with separately prepared neutrophils are presented. (F) Peritonitis was induced in *Ptpn22*$^{-/-}$ (ko) and wild-type control (wt) mice by injection of thioglycollate containing broth. Peritoneal flushes were analyzed to enumerate numbers (means ± SEM) of peritoneal neutrophils. A representative experiment performed with 6 controls and 5 *Ptpn22*$^{-/-}$ mice is shown. Differences were not statistically significant.

Europe PMC Funders Author Manuscripts

Europe PMC Funders Author Manuscripts

Table I

Ptpn22$^{-/-}$ mice are protected from K/BxN arthritis.

Irrespective of the gender of the recipient and of disease induction with a single, or repeat injections with arthritogenic serum, *Ptpn22*$^{-/-}$ mice were characterized by slower disease progression and reduced peak amplitude.

Recipient	*N*	Treatment	Mean time to peak	Mean maximal score ± SD	Time at peak intensity	Median clinical score
wt female	9	75μl on day 0	6.2 days	8.6 (±1.9)	2 days	3.8
ko female	9	75μl on day 0	6.8 days	5.0 (±1.9)	3.4 days	2.3
wt female	4	100μl on day 0, 100μl on day 2	5.8 days	10.25 (±1.6)	4 days	8.25
ko female	3	100μl on day 0, 100μl on day 2	7 days	6.0 (±1.7)	3.7 days	3.0
wt male	6	100μl on day 0	4.2 days	9.8 (±1.6)	2.3 days	4.0
ko male	6	100μl on day 0	6.7 days	6.5 (±2.9)	3.3 days	3.3